Pure appl. geophys. 157 (2000) 1683–1705
0033–4553/00/101683–23 $ 1.50 + 0.20/0

Pure and Applied Geophysics

Seismicity of the Indian Peninsular Shield from Regional Earthquake Data

BHUPESH KUMAR GANGRADE[1] and SANAT KUMAR ARORA[1]

Abstract—In this comprehensive study of seismicity and seismotectonics of the peninsular Indian shield region, seismic data of regional earthquakes spanning two decades (1978–1997), obtained at Gauribidanur seismic array (India) and integrated where necessary with data from other seismological stations in the region, have been analyzed in detail. With a slow rate of stress accumulation, the shield is found to have low to moderate seismicity that takes into account a couple of earthquakes of magnitude slightly larger than 6. The frequency-magnitude analysis of the data set gives a *b* value of 1.18. The spatio-temporal pattern of occurrences of the earthquakes combined with their magnitude and seismic energy distribution is consistent with the view that the peninsular seismicity is low to moderate and episodic in nature. Regions of moderate seismicity and its low-grade counterpart constituted by microearthquakes (magnitude less than 3), appear correlated to the areas traversed by known geologic faults and subfaults, shear zones, and other such tectonic features. Microearthquakes represent about two-thirds of the total regional seismic events during the past two decades.

Key words: Duration magnitude, regional seismicity, peninsular India, clusters, seismotectonics, Deccan plateau, earthquakes.

1. Introduction

The Indian peninsula is one of the oldest Archaean shield regions of the world. Such shield regions of the continental interiors are generally recognized as seismically stable, being either devoid of any major seismic activity or characterized by very long time intervals, of the order of centuries and millenniums, between two strong earthquakes. However, due to the occurrence of micro to moderate earthquakes in the peninsular region over the past few decades, the region should no longer be regarded as totally aseismic in nature and its seismicity requires closer study.

A slow and steady accumulation of seismic energy seems to be occurring in this region in an episodic manner, leading to earthquakes of moderate to significant magnitude. The elastic strain energy released in these earthquakes is basically a part of the intraplate seismicity arising largely out of the northeastward collision-course

[1] Seismology Division, Bhabha Atomic Research Centre, Mumbai 400 085, India.

movement of the Indian plate, crossed by faults of various sizes where the elastic stresses build up and drop periodically. It is also possible that the processes responsible for the intraplate seismicity could originate from continental margins, differential crustal movements and hot spots. In other regions like North America, Western Europe and Australia, such seismicity has been found to occur in a compressional strain environment. The collision of the Indian plate against the Tibetan block provides precisely such an environment, a potential source of accumulation of strain energy.

As a consequence of the collision of the Indian plate with the Tibetan plate, zones of weaknesses continued to be developed southwards, starting from the Indus-Tsangpo suture in the Early Tertiary. This activity perhaps in its latest phase has resulted in the underthrusting of the peninsular shield below the Indo-Gangetic plains with the age of the intercratonic subduction decreasing from north to south.

The so-called ''shield'' areas of peninsular India must be reconsidered in light of their presumed ''stability.'' The tragic consequences of the Latur earthquake of 1993, in the backdrop of the low seismic hazard previously assigned to this region, indicate that our understanding of seismogenesis of the stable continental interiors (SCI) must be reviewed. Negative paleoseismic results from the Latur region, as also those from other provinces, suggest that not only the earthquake catalogues, but also some of the known geologic features may not easily reveal potential sources of future earthquakes. A recent earthquake registering $m_b = 6.0$ which occurred on May 22, 1997 near Jabalpur (23°N, 80°E) was a manifestation of intraplate seismicity along seismically active Narmada-Son lineament. Unfortunately, the peninsula is also very sparsely instrumented at present to study its seismicity in greater detail. Nevertheless, using the data obtained mainly from Gauribidanur Seismic Array (GBA) along with those from other independent seismographic stations in peninsular India, an effort in this study has been made to investigate the seismicity of the peninsular region.

2. Salient Geotectonic Features of Peninsular India

A tectonic map of the Indian peninsula (after VALDIYA, 1973) shows major fault zones, thrusts, structural trends, granitic intrusions and the various lithotectonic provinces (Fig. 1). Archaeozoic rocks are predominantly granites and gneisses, schists (in Dharwar), igneous and sedimentary rocks metamorphosed to varying degrees. Overlying Archaeans are the Proterozoic (Precambrian) rocks belonging to the Cuddapah sediments which consist of shales, slates, quartzites, limestones and sandstones. These rocks occupy depressions of the late Precambrian times, which were formed due to faulting along their margins. The arcuate shaped Cuddapah sedimentary basin evolved on the east coast side at 15° parallel.

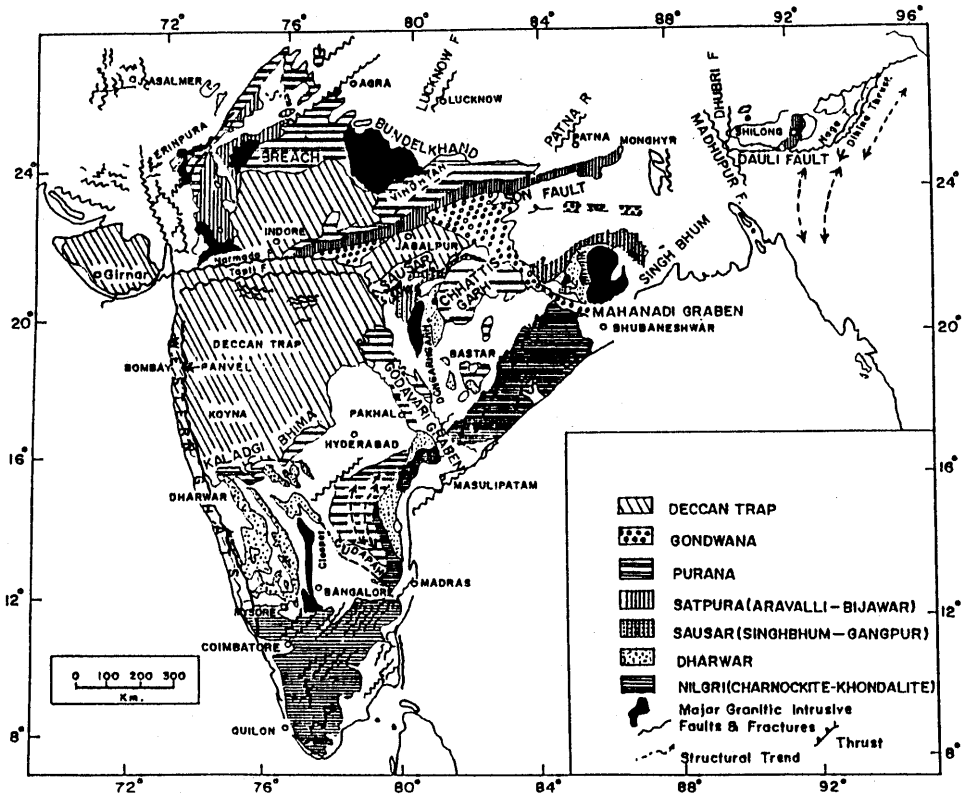

Figure 1
Tectonic map of peninsular India (after VALDIYA, 1973) showing major fault zones, thrusts and lithotectonic provinces. Blank part in Andhra Pradesh and Karnataka are mostly gneisses.

The upper Palaeozoic-Mesozoic rocks in the peninsular region occur mainly in elongated graben-type basins and are classified under the Gondwanas. They are: (1) The NW–SE trending Mahanadi and Godavari grabens towards the east coast, and (2) ENE–WSW trending Satpura Damodar graben. These grabens were initiated during the late Palaeozoic times and the sedimentation continued through the close of the Mesozoic era.

Approaching the beginning of the Cenozoic era, an intense volcanic activity began in which there were substantial outpourings of lava spread over several phases in the western part of peninsular India. These lava flows around 65 Ma (Upper Cretaceous-Eocene) solidified forming distinct beds, one over the other, and gave rise to what is now known as the flood basalt region where the overlying rocks are called Deccan Traps. The total thickness of Deccan Traps could be several hundred meters. Most of the lava flows of Deccan plateau are nearly flat lying and show little evidence of deformation. Similarly, along the eastern peninsular margin, the NE–SW trending Eastern Ghats were formed due to orogenic activity. The

coastal strips are mostly covered by Tertiary shelf deposits. The western margin of the peninsular shield is bounded by a great N–S scarp, and the northern margin is fractured and folded in the E–W direction along the Satpura range.

During the formation of the Deccan Traps, the lava which flowed on the already elevated Western Ghats resulted in forming variable dip and slope to the province. This westerly dip is due to monoclinal flexure which was named the Panvel Flexure (AUDEN, 1949). It lies roughly between 16°N to 21°N and 73°E to 74°E, striking in the NNW–SSE direction. This flexure development is associated with the West Coast Fault (WCF) which parallels the edge of the continental shelf (DESSAI and BERTRAND, 1995). The WCF and Panvel flexure could be a manifestation of the stretching, fracturing and breaking of continental lithosphere in response to rifting. However, BURKE and DEWEY (1973) regarded this fracture system as running parallel to one arm of the triple junction located around Cambay (22.3°N, 72.6°E).

Peninsular India is thus traversed by numerous faults and tectonic lineaments. Major lineaments observed in the region include the NW–SE, NE–SW, NNW–SSE and WNW–ESE trending sets (RASTOGI, 1992a). Evidence from geological data suggests that some of these faults and lineaments are very old, being of Precambrian origin, whereas others are comparatively much younger and possibly of neotectonic origin. Many of these faults seem to have ruptured independent of each other at different times. Most of such asperities are also known conveying intersections from transverse structural trends.

3. Brief Description of Gauribidanur Seismic Array and Catalogue Preparation

GBA is one of the four arrays set up by United Kingdom Atomic Energy Authority (UKAEA), UK. The other three are Warramunga seismic array (WRA) in Australia, Yellowknife seismic array (YKA) in Canada and Eskdalemuir seismic array (EKA) in Scotland. GBA is an L-shaped medium aperture array with ten seismometers in each arm (Fig. 2). Each pit of the array is designated as R1-R10 along one arm and B1-B10 along the other arm. The seismometers (velocity transducers) are kept at a distance of 2.5 km from one another. The Central Recording Laboratory (CRL) is located at B1 which is the crossover point of the array where all the data from 20 seismometers are received and recorded on magnetic tapes and one channel is also displayed on helicorder. The seismic network has basically remained unchanged during the twenty-year period (1978–1997) of data considered for analysis. The main changes are in the computerization of data recording at the CRL and the introduction of wireless telemetry rather than cable telemetry in some pits.

From the multichannel-recorded seismograms of an event we obtain P and S arrival times, the time lags in the two arms and the total signal duration. These are

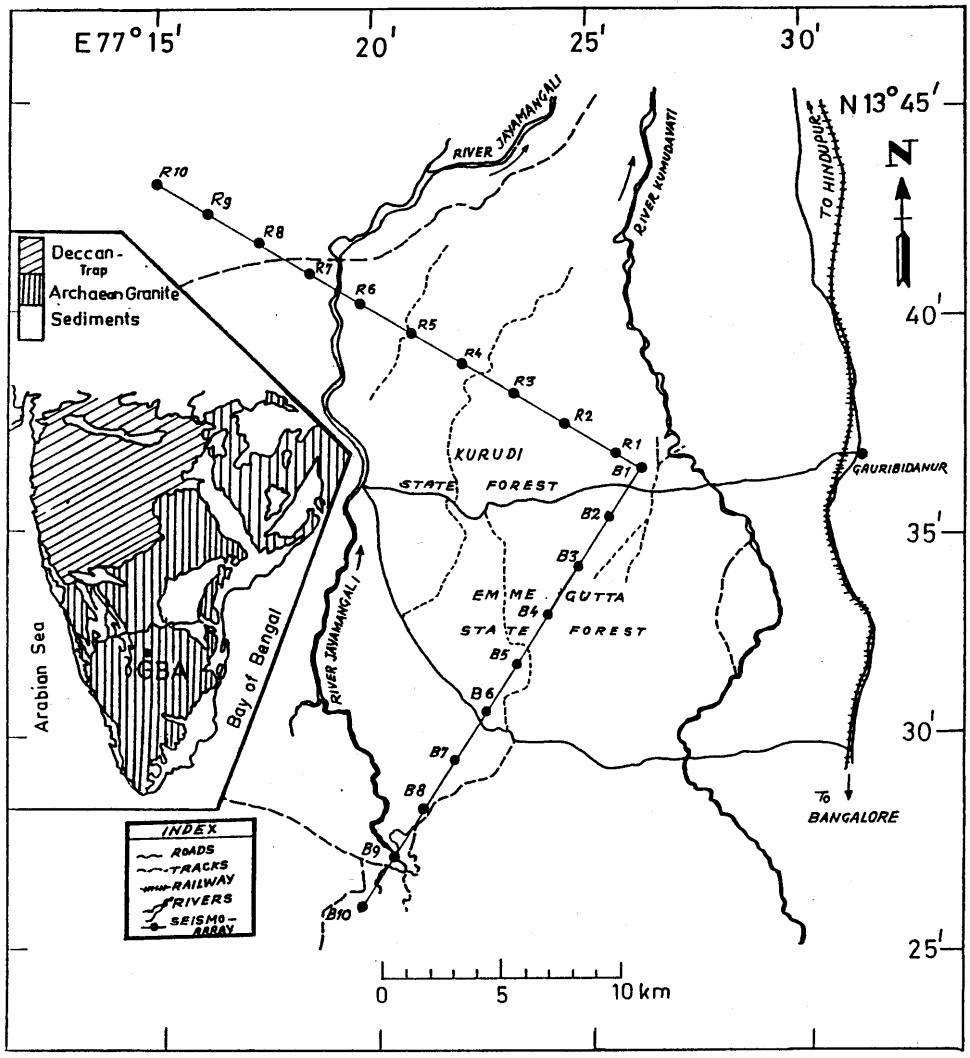

Figure 2
Layout of the Gauribidanur seismic array showing the two red and blue arms perpendicular to each other.

employed to extract the required parameters of an event viz. origin time, azimuth and epicentral distance (which give latitude and longitude of the event), and the duration magnitude of the event as described below. All the events, which fall within a distance of about 1000 km around GBA, have been taken for the present study and catalogued.

4. Event Magnitude Based on Signal Duration

We have evolved an empirical relationship for estimating the magnitude of a regional seismic event based essentially on signal coda duration (τ) and epicentral distance (D). This relationship has been obtained by regression analysis of body-wave magnitudes (m_b) of the earthquakes reported in the PDE (Preliminary Determination of Epicenters), published by the USGS (United States Geological Survey), and in the catalogues of ISC (International Seismological Centre, UK) against the governing parameters extracted from the seismograms of GBA (GANGRADE and ARORA, 1996; GANGRADE *et al.*, 1994). The following expression was used to obtain the regression coefficients $a1$, $a2$, $a3$:

$$m_b = a1 + a2 \log \tau + a3 \log D \tag{1}$$

where τ is the total signal duration in seconds and D is the epicentral distance in km. HERRMANN (1975) and REAL and TENG (1973) have used D instead of $\log D$ in relation (1). In our case, since the maximum epicentral distance being considered is approximately 1000 km, it results that M_τ are closer to m_b when $\log D$ (instead of simply D) is used. The expression for the GBA duration magnitude, M_τ, thus obtained is as follows:

$$M_\tau = -3.62 + 2.51 \log \tau + 0.37 \log D. \tag{2}$$

This relation can also be applied to stations with instrumental constants comparable to those of GBA. The applicability of relation (2) can be extended to other stations by adding an appropriate correction term to account for attenuation with regard to signal amplitude and coda compression, normalizing with reference to GBA.

Figure 3 displays the calibration of M_τ against m_b. The solid line is the linear regression line between duration magnitude and body-wave magnitude. The regression line has been passed through zero. The value of standard deviation (σ) is 0.34. The two dashed lines are one standard deviation from the regression line. The agreement between the two magnitudes seems reasonably good up to $m_b = 5.5$, there being an insufficient number of earthquake occurrences in peninsular India to provide such data in the larger magnitude range. If a larger data set covering a wide range of magnitudes becomes available, it should reduce the scatter tending to improve the duration magnitude relation.

5. Earthquake Data and Seismicity of Peninsular India

In the present study, seismic events which occurred in peninsular India in the past twenty years (1978–1997) have been considered. In addition to GBA, wherever possible, data from other regional seismic stations viz., Hyderabad (HYB: 17.42°N,

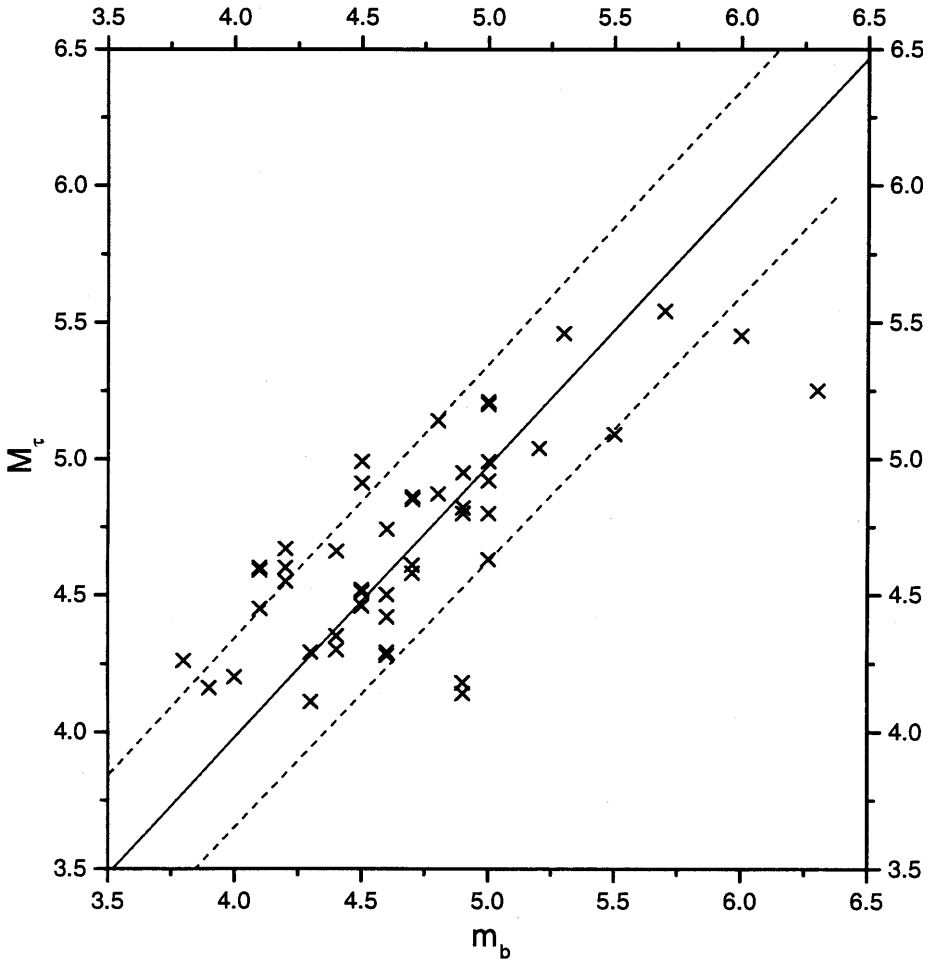

Figure 3
Estimated duration magnitudes, M_τ, are plotted (shown as crosses) against the body wave magnitudes, m_b. The solid line is the linear regression line whereas the two dashed lines are at a distance of one standard deviation from the linear fit.

78.55°E), Poona (POO: 18.53°N, 73.85°E) and Kodaikanal (KOD: 10.23°N, 77.47°E) have also been pooled to improve seismicity study.

It is important to note that seismic events corresponding to presumed mine blasts associated with iron-ore mining operations in Sandur, Hospet, Bellary and Kudremukh areas as well as frequent rockbursts occurring in the gold mines at Kolar Gold Fields (KGF) have been kept out of this study since they all constitute events of non-tectonic origin. There are reports of only three earthquakes of some consequences with a maximum intensity of VII on the Modified Mercalli (MM) Scale in peninsular India in the historical past (CHANDRA, 1977). These occurred at

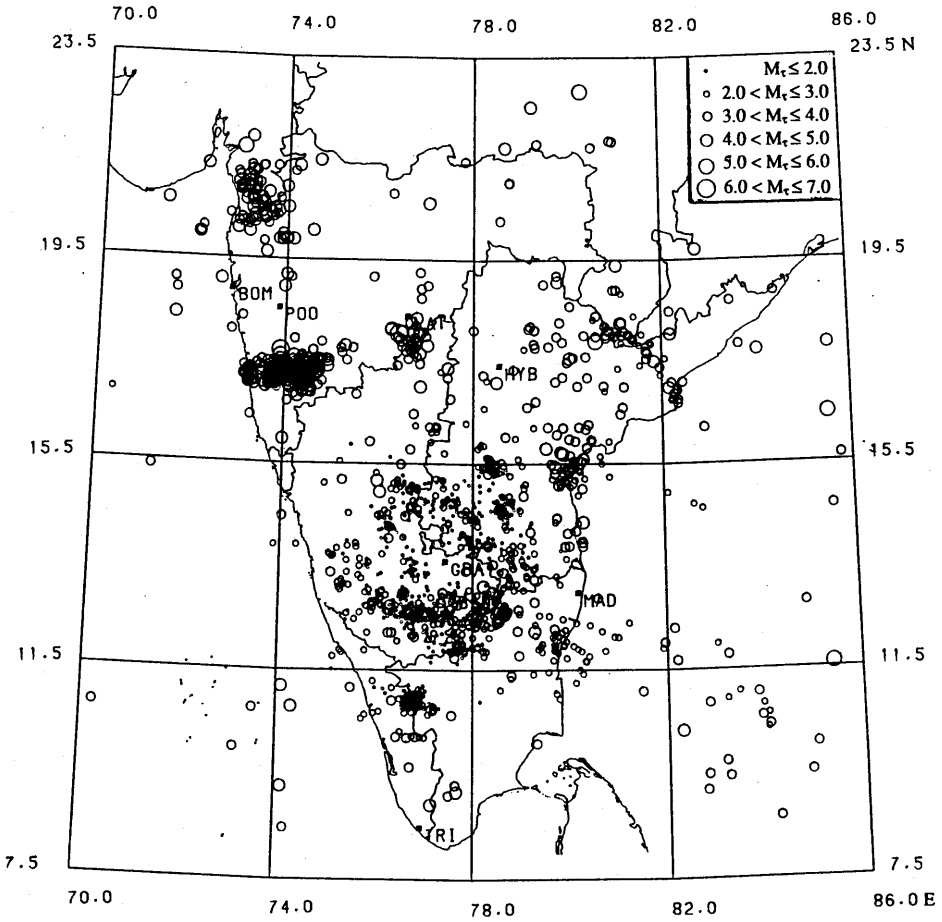

Figure 4
Typical seismicity of peninsular India based on mainly Gauribidanur seismic array (GBA) detections of regional earthquakes spanning two decades (1978–1997). The epicenters are designated by open circles whose radii are proportional to the estimated magnitude of the earthquakes (see legend).

Mahabaleshwar (1764), Bellary (1843) and Coimbatore (1900). Apart from these three events, there have been a few earthquakes of intensities IV and V on the MM scale. It is only in recent decades that the occurrence of some earthquakes of $m_b > 5$ and a couple of earthquakes of $m_b > 6$ has caused concern which led to the study of peninsular seismicity in greater detail. However, attempts to correlate seismic events with various tectonic features are few, probably due to its low seismic activity (CHANDRA, 1977; RAO and RAO, 1984). Figure 4 shows the spatial distribution of regional earthquakes detected by GBA. The epicentral locations of the events obtained by using GBA data alone are satisfactory. However, these source locations show definite improvement where data from other regional seismic

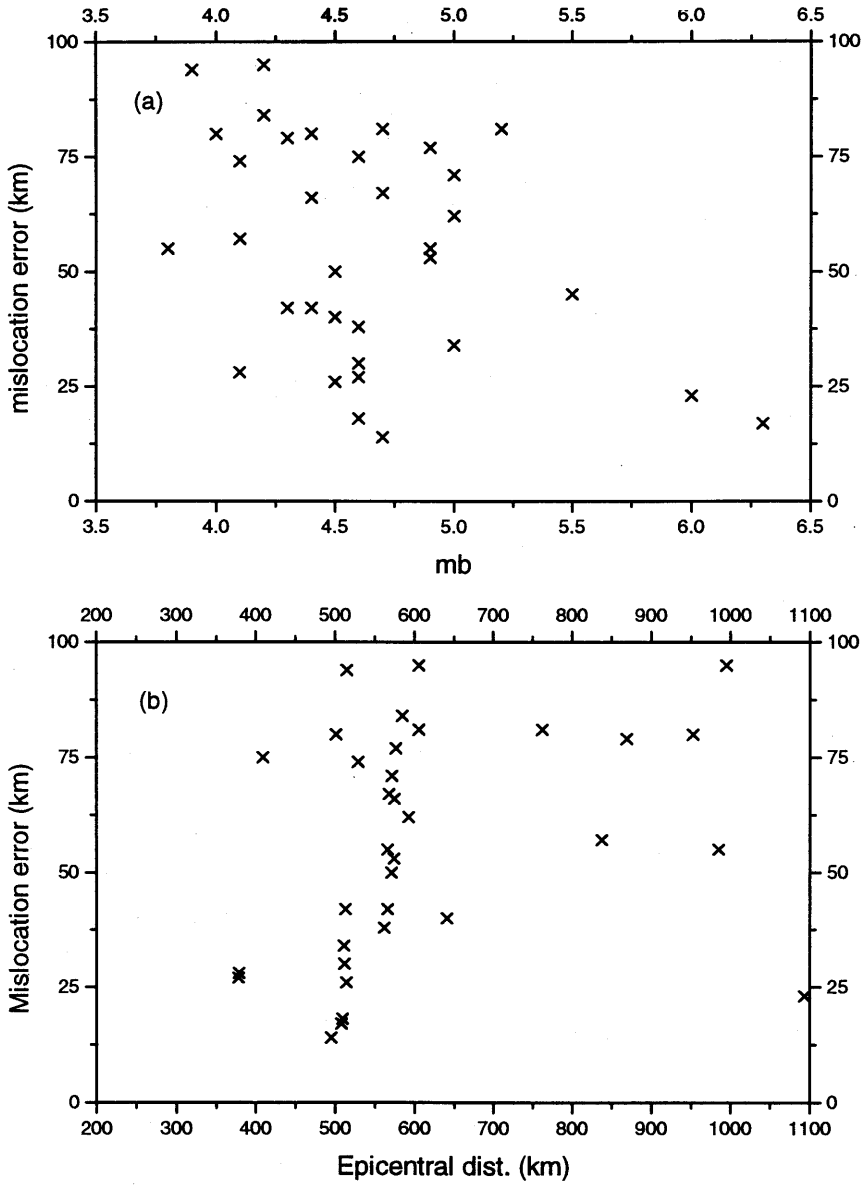

Figure 5
Mislocation error is shown as crosses with respect to (a) m_b and (b) epicentral distance.

stations become available. The mislocation errors are not found to depend directly on either the magnitude of the event or the epicentral distance (Figs. 5a and 5b), nonetheless they are certainly influenced by the accuracy with which input parameters from the seismograms are obtained (GANGRADE *et al.*, 1987a,b, 1989, 1992).

The comparison of the epicentral locations obtained by us with the locations given in the PDE and ISC demonstrates that the errors in epicentral distances vary from as small as 10 km to as large as 90 km.

In order to make a comprehensive evaluation of the seismicity of a given craton however, it is required to have considerably more seismic stations uniformly distributed over the mosaic. In the seismicity map of Figure 4 we notice, apart from some distinct clusters of earthquakes in specific locations, several scattered events which imply low to moderate seismic character of the peninsular shield. The illustration in Figure 6 shows that most of the microearthquakes (magnitude $M_\tau \leq 3$) detected by GBA, sometimes in association with other local seismic stations, are located within roundly 400 km from GBA, marked by a circular area thereon. Even though such low magnitude events may also be occurring in other

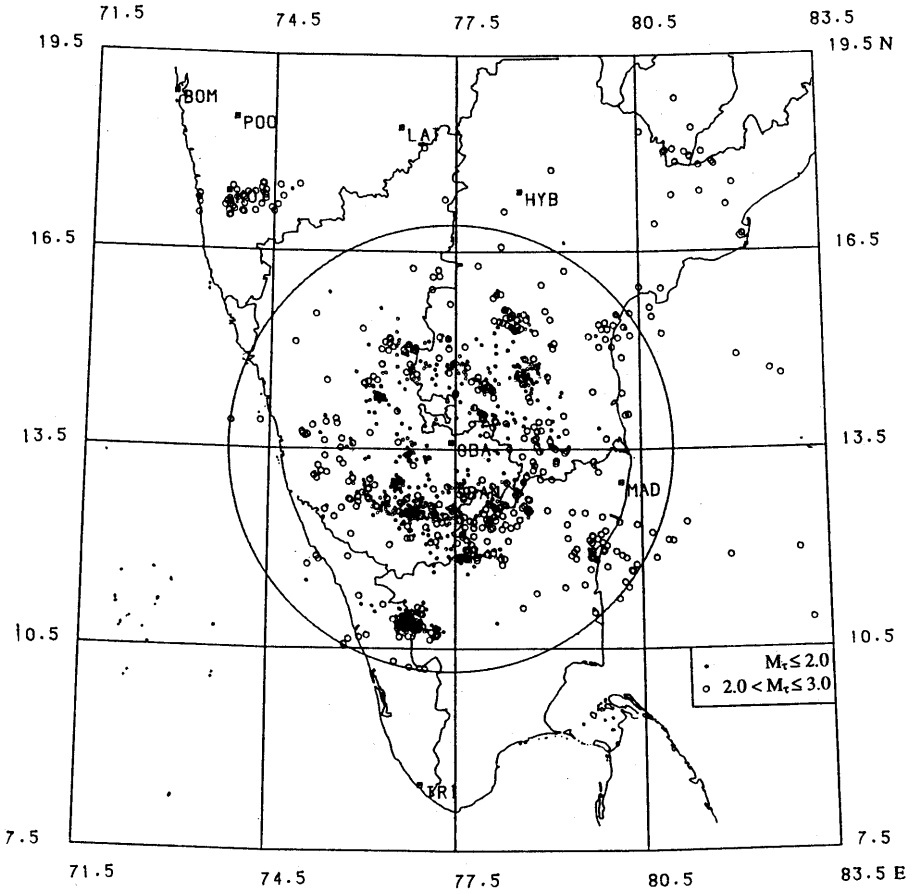

Figure 6
Distribution of sources of microearthquakes (magnitude $M_\tau \leq 3.0$) detected by GBA. Other details are the same as in Figure 2. The large circle centered at GBA is of 400 km radius.

distant parts of the shield, they are not detected by GBA and therefore do not find a place in these illustrative maps. Nevertheless, microevents of small magnitude ($M_\tau \leq 2$) are seen to be bunching within a distance of about 300 km around GBA. This also bears upon the monitoring capability of GBA with respect to regional earthquakes. The occurrence pattern of events is found to either conform to clusters or they are scattered as shown clearly in Figure 4. Below we discuss seismic characteristics of the regions of earthquake events.

5.1 Koyna Region

Centered around 17.3°N, 74.0°E (Fig. 4), this region is well known for the occurrence of Reservoir-Induced Seismicity (RIS). The largest magnitude earthquake ($m_b = 6.5$) that occurred in this region of Shivajisagar Lake, which has a high dam was on December 10, 1967. Since then, for more than thirty years the region has been constantly experiencing earthquakes. Some earthquakes ($M_\tau \geq 5$) occurred in this region during September–October, 1980. Other sequences, although of relatively less intense activity ($3 < M_\tau < 5$), were again recorded in 1993 and in 1996.

It is seen from the figure that the events around Koyna show some spread rather than being localized. This scatter is attributed largely to inaccuracies in source location as has been explained earlier. From the Koyna region, the majority of events detected by GBA are of magnitude $M_\tau > 3$. However, Maharashtra Engineering Research Institute (MERI), which has set up instruments to monitor local seismicity of Koyna and its surrounding region, does report a large number of microearthquakes occurring in that region. The activity follows two major trends: One is along a NNE–SSW trend near the reservoir, where the majority of the earthquakes have occurred and the other is a NW–SE trend cutting across the NNE–SSW trend. Composite focal mechanisms obtained for earthquakes show strike-slip faulting for the NNE trend and normal faulting for the NW trend. The area of intersection of these two trends appears to be most active (GUPTA, 1985, 1992).

5.2 Khardi-Bhatsa Region

Its center located at 19.9°N, 73.9°E (Fig. 4), the Khardi-Bhatsa region lies close to Bhatsa reservoir which has a large masonry-gravity dam some 80 km northeast of Mumbai. Seismic activity initially spurted in this region in 1983–1984, a few years after impoundment of the Bhatsa reservoir. The largest earthquake of $M_\tau = 4.9$ (largest detected to date from this region) occurred on September 15, 1983, and was associated with some felt foreshocks and a number of aftershocks (ARORA *et al.*, 1989). After a gap of nearly six years, on June 2, 1990, another event of $M_\tau = 4.1$ took place, preceded by microforeshocks and followed by small

aftershocks. This activity, gradually tapering off within about four weeks with a tendency to return to normal, had characteristics of a swarm.

It has been noted that the 1983 earthquake sequence followed a rapid rise of water level in the reservoir by 18 meters, leaving one strongly suspecting it to be a case of RIS. On the other hand, the 1990 activity took place when the water level in the reservoir was at its minimum. This negative correlation of earthquake occurrences with the water level standing at its lowest in the season, however, does not rule out the possibility of a delayed RIS. Apart from these two seismic sequences (1983–1984 and 1990), the region has experienced sporadic microtremors of shallow foci (depths of less than 5 km) and located mostly in and around the reservoir. Earthquakes of magnitudes $3 < M_\tau < 4$ have been infrequent and located away from the reservoir area. All these data have come from a radio-telemetered local seismic network installed at Bhatsa by the Bhabha Atomic Research Centre (BARC) in 1988 (KOLVANKAR *et al.*, 1992).

The region is crossed by the NW–SE trending Kalu-Surya fault system, Talekhan fault and Kengri Nadi lineament which are responsible for the above seismic activity. These faults are essentially parts of Ghod megalineament, subparallel to the Panvel flexural axis. For the Bhatsa sequence the composite fault plane solution indicates right-lateral strike-slip, with down-dip normal movement along a NNW trending nodal plane (RASTOGI, 1992a).

Although the cases of Bhatsa and Koyna both are considered as those of probable RIS, there are two basic differences in their seismicities. In Koyna, of a multitude (thousands) of events that have occurred there after the 1967 main earthquake, the magnitudes range to 5.8, averaging around 4. At Bhatsa, most of the events are in the microearthquake range and the number of earthquakes is substantially less as compared to Koyna.

5.3 Broach-Valsad Region

The earthquake sources near Broach in Gujarat centered around 21.0°N, 73.0°E and that near Valsad around 20.4°N, 73.5°E are shown in Figure 4. This region is some 100 km to the south of the Narmada-Tapti rift zone which runs nearly in a E–W direction which divides the shield into two parts along a 22 degree parallel (KHATTRI, 1994). An event of $m_b = 5.4$ occurred on March 23, 1970 in the Broach depression lying between the Dharwar craton to the south and the Aravalli craton to the north. The Broach earthquake source region also coincides with the confluence of three well-known faults, namely the SONATA (Son-Narmada-Tapti) rift zone, the Aravalli fault and the West Coast fault (ARORA *et al.*, 1971). The earthquake sources clustered in this region seem to broadly follow the same seismotectonic pattern as the one that applies to the 1970 Broach earthquake.

Juxtaposed to the Broach region, the Valsad region experienced seismic activity in 1986, with the largest event of magnitude $M_\tau = 4.6$ (April 27, 1986) followed by

several small earthquakes. According to RASTOGI (1992a), for the Valsad earthquake sequence the composite fault plane solution indicates normal faulting mixed with right-lateral strike-slip movement along the NW–SE trending fault plane, which is consistent with the NW–SE trending lineaments mapped in this area. Lineaments trending NE–SW are also present in the region. The E–W trending nodal plane could also be the fault plane which is in the direction of the SONATA rift zone. Perhaps activation of one of the branches of the triple junction located around Cambay as described earlier could also have been a causative element in the earthquake occurrences in this region.

5.4 Latur Region

Centered around 18.0°N, 76.6°E close to Killari (Fig. 4), this cluster came into being after the strong earthquake ($m_b = 6.3$) that struck the Marathwada region of South-Central Maharashtra early in the morning (local time, IST) on September 30, 1993 (September 29, 1993 according to GMT). This event registered intensity IX on the Modified Mercalli (MM) scale and the meisoseismal area enclosed approximately 150 km^2 in and around the Tirna valley, with a focus at an estimated depth of less than 10 km. Widely felt in Mumbai (Maharashtra) and the bordering areas of Karnataka and Andhra Pradesh, this Latur-Osmanabad earthquake has been the most devastating earthquake that occurred in the SCI of peninsular India (see, ARORA, 1994). The Latur-Osmanabad area, belonging to the Deccan volcanic province (DVP), was demarcated as Zone I by the Bureau of Indian Standards (BIS), which is due to be appropriately upgraded now. Several zones of weakness below the Deccan Traps have been hypothesized and they are poorly identified. Nevertheless, brittle faults are common in exposed basement worldwide and the Latur event took place on such a preexisting fault buried below the Deccan basalts (SEEBER *et al.*, 1996).

The region of sudden outbreak of this intense seismic activity is not known to have sustained any major earthquakes in the historical past. However, there was a spurt of activity interestingly around the same period in the preceding year (October–November, 1992) when an earthquake of $m_b = 4.5$ occurred in the vicinity of Killari (which is located approximately 30 km east of Latur) on October 18, 1992, followed by small aftershocks. With no immediate foreshocks detected, the main earthquake of September 30, 1993 gave rise to a large number of aftershocks which essentially constitute the Latur cluster.

A WNW–ESE striking and NNE dipping basement fault below the Traps is inferred to be the causative fault activated by a predominantly thrust type of focal mechanism (GUPTA, 1993). The epicentral region is characterized by gravity low, which is considered to have a trend relationship with the well established Kurudwadi Rift system (KRISHNA BRAHMAM and NEGI, 1973).

5.5 Bhadrachalam Region

Earthquakes in this region are located around 18.0°N, 81.0°E (Fig. 4). The earthquake locations obtained using GBA data, integrated with those from other stations, are slightly northeast of the town of Bhadrachalam in Andhra Pradesh. A moderate earthquake of magnitude 5.3 occurred on April 13, 1969 in this region, following which the rate of occurrence of aftershocks decreased rapidly. All these events have been thoroughly studied by ARORA *et al.* (1970), and they were in crustal focus with hypocentral depths less than 20 km. The long and narrow Godavari Rift oriented NW–SE, which forms the contact between the two major cratons, namely Dharwar and Singhbhum cratons, is the causative fault that generated the main April 13, 1969 earthquake and its aftershock sequence.

Since then only small earthquakes from this region are occasionally detected by GBA. This seems to indicate that the region is seismically not very active, the activity there being of minor nature. Excepting a few events of duration magnitudes $M_\tau > 4$, the majority of the earthquakes are $3 < M_\tau < 4$. The fault plane solution of the main event indicates a left-lateral strike-slip motion along NE striking faults (RASTOGI, 1992b).

5.6 Ongole Region

Lying on the east coastal boundary and centered around 15.3°N, 80°E (Fig. 4), this region experienced an earthquake of magnitude $m_b = 5.4$ on March 27, 1967, to date the largest in this region. Barring a few earthquakes of $4 < M_\tau < 5$, only minor tremors have been recorded from this region. All the events originated within a small area in the NE–SW trending zone. The fault plane solution indicates predominantly left-lateral strike-slip movement along the NE striking fault (RASTOGI, 1992b).

5.7 Coimbatore-Palghat Region

This region located close to 10.9°N, 76.9°E is known to have witnessed in the historical past an earthquake of magnitude 6 in the year 1900 (KRISHNA BRAHMAM and KANUNGO, 1976). The source of this event was estimated at a rather large depth of 70 km unlike other earthquakes in peninsular India, all of which have hypocenters in the upper crust. Subsequently, in 1972, the activity recurred engendering an earthquake of magnitude 5. Since then, as shown in Figure 4, mainly microtremors ($M_\tau < 3$) have been recorded from this region. The Coimbatore-Palghat area is surrounded in the west by the NNW–SSE trending Kerala fault, in the north by the ENE–WSW trending Bhavani fault and in southeast by the NE–SW trending extended Attur fault (VALDIYA, 1989).

5.8 Pondicherry Region

The East Coast boundary fault trending NE–SW traverses this region which is centered around 12.0°N, 79.7°E. Largely concentrated near Pondicherry, most of the earthquakes in this region record magnitudes less than 3 (Fig. 4), which indicates that the region is mildly seismogenic.

5.9 Arcot Region

About 200 km southeast of GBA, this region is located around 12.7°N, 78.7°E (Fig. 4). It lies in the well-known Transition Zone (TZ) of peninsular India, described for instance, by RAO (1992). It is bounded on the north by low-grade greenstone-granite terrain and on the south by high-grade granulitic terrain. The contact between these two terrains is gradational. The diffused and weak seismicity in the TZ could be attributed to reactivation of the adjoining shear zones. The estimated magnitudes of some of the earthquakes in this region range $3 < M_\tau < 4$, while the majority of them have been of smaller magnitudes ($M_\tau < 3$).

6. Seismic Event Distribution

We know that the number of earthquakes occurring in a tectonic block in a given timeframe (also termed as frequency) and their magnitudes are interlinked. For the peninsular Indian block as a whole, using two decades (1978–1997) of data, the variation of seismic count (N) with respect to duration magnitude (M_τ) can be seen in Figure 7, grouped in a range of 0.5 units of magnitude. From the histogram it is seen that most of the regional earthquakes recorded at GBA range in the magnitude $1.5 < M_\tau \leq 2.0$. This is because GBA detects a large number of microearthquakes close to it. The number of events in the range $2 < M_\tau \leq 4$ is relatively small and remains practically constant at about 50–60 events annually.

Figure 8 shows the yearly distribution of the number of regional earthquakes detected mainly by GBA. During the years 1978–1979 only partial compilations of GBA data of regional earthquakes were available, and therefore the number of events in the initial part of Figure 8 appears small. During 1980 the number shot up due to a sudden increase in activity at Koyna. For the next three years, 1981–1983, the seismicity was at nearly the average seismic level. During the years 1984 and 1986 it rose to a higher level because several small earthquakes occurred in the Bangarapet and Srirangapattanam areas in 1984, and the Valsad activity dominated in 1986. Thereafter no significant fluctuation is noticed in the recorded number of events. A gradual step-wise increase in the seismic activity beyond 1992 (1993 to present) is, however, attributed to the September 30, 1993 Latur earthquake ($m_b = 6.3$) and its aftershocks, and to the earthquake activity in the Koyna

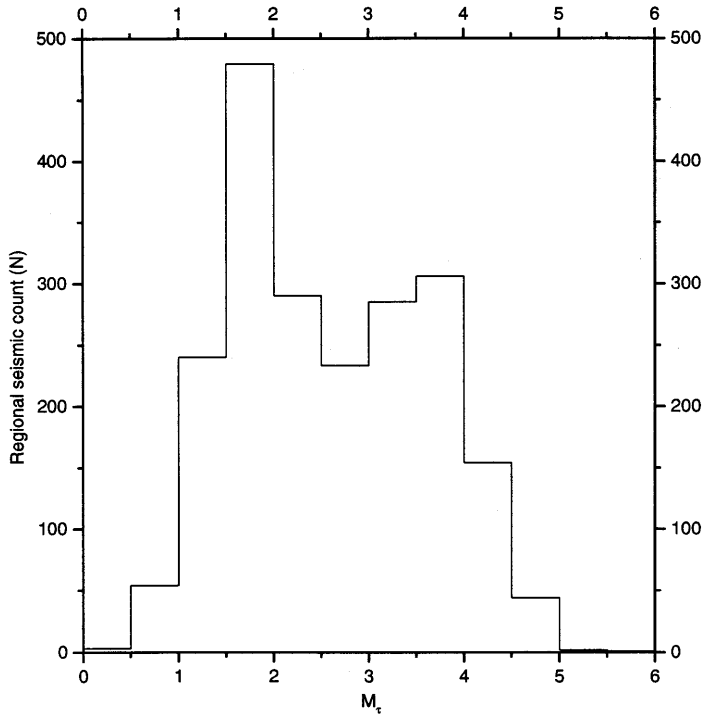

Figure 7
Magnitude distribution of the regional earthquakes in the entire data set (1978–1997). Events are grouped in the magnitude interval of 0.5 M_τ units.

region which takes place intermittently. During 1996–1997 the number of events seen are relatively less due to technical reasons.

The cumulative seismic count (ΣN) as a function of time since 1978 compared with a profile for N is shown in Figure 9. The ΣN data were subjected to general least-squares fitting through polynomials of various orders, starting from the linear fit. The difference between them in terms of departure from the linear fit was found to be insignificant. Hence, for simplicity, we choose the linear trend for which the expression is as follows:

$$\Sigma N = -190.74 + 105.49t \tag{3}$$

where the time t is in years. The linear ΣN: t relationship in peninsular India examined over a period of 20 years, in which a major earthquake (1993 Latur earthquake) is also included, suggests that the peninsular seismicity is moderate and at times manifests sporadic although relevant events. These features are noteworthy since they provide important inputs in the assessment of the seismotectonic status of the region. Nevertheless the seismic potential of each of the earthquake-prone provinces in the peninsular block must be mapped separately in detail for zonation of seismic hazard.

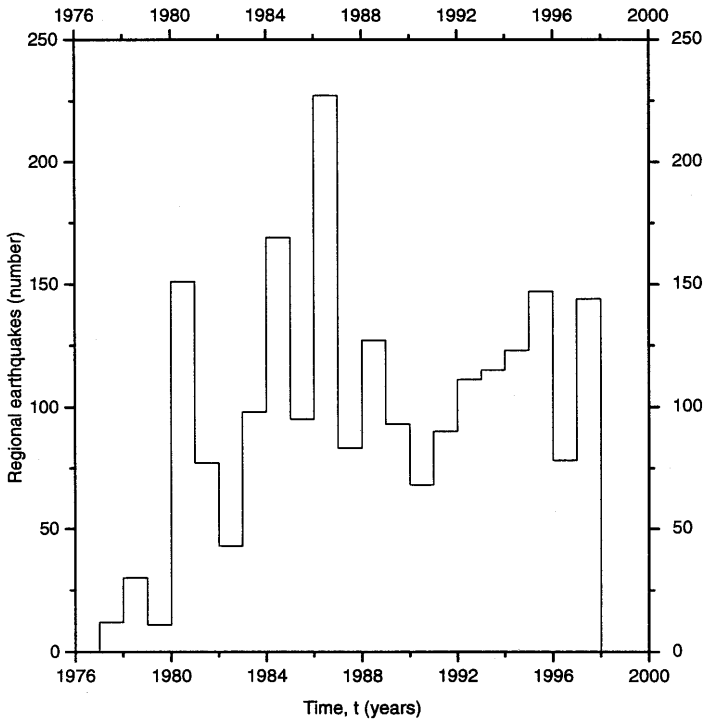

Figure 8
Temporal distribution of the regional earthquakes starting from the year 1978, taking the unit of time as one year.

7. Magnitude and Energy Distribution

The empirical relationship between the elastic strain energy, E, released by an earthquake of magnitude M takes the following form:

$$\log E = K_1 + K_2 M \tag{4}$$

where K_1 and K_2 are empirical constants. In general, different values of K_1 and K_2 have been obtained, depending on whether a body-wave magnitude (m_b), local magnitude (M_L) or surface-wave magnitude (M_s) has been considered for energy calculation. Since we have used m_b values for obtaining the M_τ relationship, the following relation (LAY and WALLACE, 1995) can very well be used for energy calculation:

$$\log E = 5.8 + 2.4 M_\tau. \tag{5}$$

The pattern of cumulative seismic energy release (ΣE) presented in Figure 10 shows a steady rise over the data period from 1978 to 1997. The relative higher steps of ΣE in the years 1980, 1986 and 1993 are consistent with the increase in

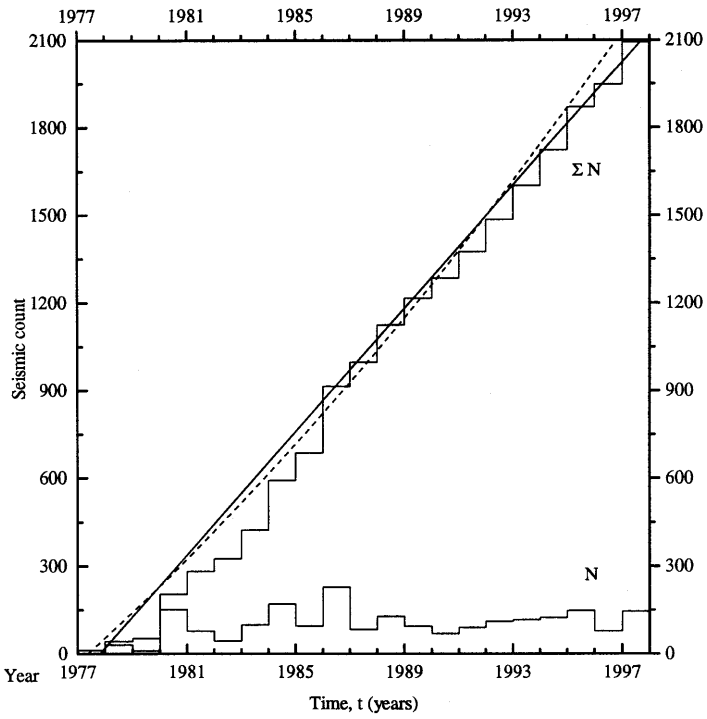

Figure 9
Cumulative seismic count, ΣN, as a function of time in years. Dashed line is the quadratic fit and the closest accepted trend is the linear fit illustrated by solid line. For comparison, the yearly seismic count N reproduced from Figure 7 is also shown.

seismic activity in those years in terms of both the number of earthquakes and the occurrence of a large magnitude event in 1993 (Latur earthquake) as explained in the preceding section. The overall pattern, however, exhibits a linear trend as evidenced by the least-squares fit through the ΣE data. The best fit, therefore, is represented by:

$$\Sigma E = -84.78 + 47.36t \tag{6}$$

where the time t is in years. This linear trend corroborates well the ΣN: t behavior seen through Figure 9 characterizing the peninsular seismicity.

8. *Frequency-magnitude Analysis*

Seismic data of GBA detections of regional earthquakes that occurred during the past two decades (1978–1997) constitute the data set for frequency-magnitude analysis using the well-known Gutenberg-Richter (GR) linear relation: $\log N = a -$

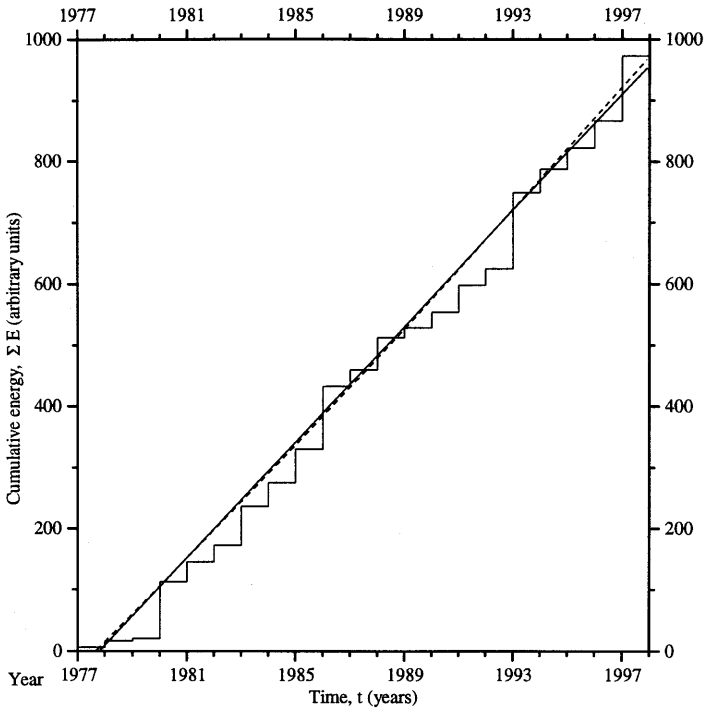

Figure 10
Temporal profile of cumulative seismic energy release, ΣE, encompassing the period 1978 to 1997. Dashed line is the quadratic fit and the closest accepted trend is the linear fit illustrated by the solid line.

bM. The cut off level of magnitude (M) is important since it largely influences the number of earthquake events (N) in a given data set, when events of magnitude M and above are considered. The constants a (intercept on $\log N$ axis) and b (slope) of the linear relation have been estimated by least-squares fitting through the entire data set. The standard deviation (σ) in $\log N$ and the correlation coefficient (ϕ), both of which reflect upon the goodness of fit, have also been estimated (Table 1).

Table 1

Estimated regression coefficients of the Gutenberg-Richter (GR) frequency-magnitude relation from 20 years' (1978–1997) GBA data of regional earthquakes

Parameter	Estimates		
	All events	Events of $M_\tau > 2$	Events of $M_\tau > 3.5$
Constant a	3.90	5.30	7.16
Constant b	0.45	0.80	1.18
Std. dev. (σ)	0.46	0.39	0.24
Corr. coeff. (ϕ)	0.85	0.91	0.96

As seen from Figure 11, as is usually the case, the cumulative count N displays saturation towards the lower end of M_τ, owing to practical limitations of event detection capability. Therefore, the linear fit through the bulk data (all events) is not expected to yield realistic estimates of the seismicity parameters. However, it is important to deduce the lower limit of magnitude above which the observed data best satisfy the linear GR relation. In the present case we took different cutoff magnitudes, starting from $M_\tau > 2$, until stability of parametric estimates was achieved. It turned out that the slope of the linear fit remained practically constant for magnitude cutoff above 3 which determines the required limit. The gradually increasing (as expected) values of the constants a and b with magnitude, as seen in Table 1 supported by the illustration in Figure 11, are consistent with the corresponding improvements in the goodness of fit (decreasing and increasing values of σ and ϕ, respectively).

Thus, with $M_\tau = 3.5$ the b value at 1.18 obtained from the large data set is considered reliable. GUPTA and RASTOGI (1976) have, however, obtained a lower b

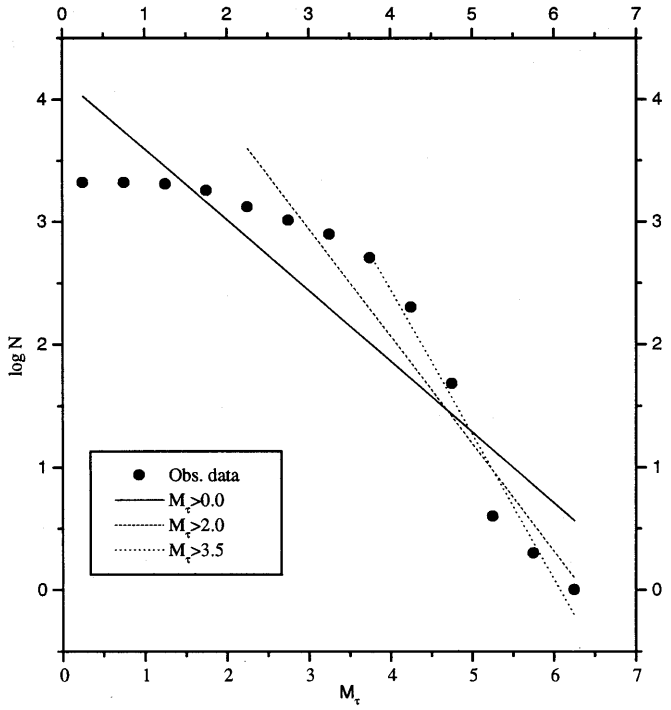

Figure 11
Frequency-magnitude relationship plots where solid circles represent observed data, solid line is the least-squares fit through all of the data ($M_\tau > 0$), exhibiting large scatter in comparison with an improved linear fit (long-dashed line) when restricted data ($M_\tau > 2$) are used, while the best fit (small-dashed line) with minimum deviation from the observed data is found in the range $M_\tau > 5$.

value of 0.47 for earthquakes in peninsular India, using historical records exceeding 300 years. This value matches with our estimate from the all-event set (Table 1) that we do not consider appropriate because their b value is based on 52 earthquakes only in the magnitude range 4.0–7.0 during the past more than 300 years prior to the year 1975.

The b value is a measure of stress in a region, the lower b value signifying higher stress field (KEBEDE and KULHANEK, 1994). Clearly, b is a statistic which measures the proportions of large and small earthquakes; if b is large, small earthquakes are relatively common, whereas when b is small, small earthquakes are relatively rare (FROHLICH and DAVIS, 1993).

9. Conclusions

This study of the seismicity of peninsular India utilizing regional earthquake data of mainly GBA spanning two decades up to 1997, reveals that the entire region is susceptible to occasional earthquakes of magnitudes ranging 5–6. Earthquakes in the Koyna region have persisted ever since the major earthquake in 1967. In parts where clusters of events have been identified, they are related to prominent faults, lineaments, grabens or rifts, whereas areas of scattered small events can be related to minor subfaults which branch from the main faults.

Reflecting on the history of the past significant peninsular earthquakes, it is observed that all of them had occurred on fresh and unknown faults, not known to have ruptured before. Hence the possibility that these tectonic lineaments which have shown no seismic activity to date, might do so sometime in the future, is not ruled out. Such possibilities have also been noticed by SEEBER *et al.* (1996).

Owing to small although practically continuous lithological readjustments taking place within the crustal volume, numerous microearthquake occurrences are observed in the region, especially in areas around GBA, for which the array detection capability is maximum. Thus, nearly two-thirds of the regional seismic count over the last twenty years comprises by microearthquakes.

Our estimates of event magnitude based essentially on coda duration and whose formulation has been calibrated with body-wave magnitude from teleseismic data are considered reliable in a magnitude ranging to $m_b = 5.5$. Above this limit the duration magnitude tends to be underestimated perhaps due to the lack of data in the larger magnitude range.

Frequency-magnitude analysis providing a b value at 1.18 characterizes the shield region and supports the deduction of low to moderate seismicity of the region.

Acknowledgements

We thank our colleagues at the Seismic Array Station, Gauribidanur for their unremitting support in systematically compiling data of daily earthquake detections. The Array Station staff also assisted in retrieving from analog and digital tapes seismograms of events not available from the on-line seismic data acquisition system. The authors are very thankful to the two anonymous referees for critically reading the manuscript and for their useful comments in its enhancement.

REFERENCES

ARORA, S. K. (1994), *The Killer Earthquake of Killari*, *Deep Continental Studies in India*, Newslett., DST *4* (2), 2–4.

ARORA, S. K., VARGHESE, T. G., and KRISHNAN, C. A. (1970), *Some Aspects of the Structure of Southern India Based on Recent Bhadrachalam Earthquakes*, Nature *225*, 261–262.

ARORA, S. K., NAIR, G. J., and VARGHESE, T. G. (1971), *Broach Earthquake of March 23, 1970*, Earthq. Not. *42* (2), 17–26.

ARORA, S. K., GANGRADE, B. K., KRISHNAN, C. A., and KOLVANKAR, V. G., *Seismic investigations in the Bhatsa dam region of western Maharashtra*, Seminar on *Earthquake Processes and their Consequences—Seismological Investigations*, *Kurukshetra* (October 31–November 3, 1989).

AUDEN, J. B. (1949), *Dykes in Western India*, Trans. Nat. Inst. Sci. Ind. *3*, 123–157.

BURKE, K., and DEWEY, J. F. (1973), *Plume Generated Triple Junctions: Key Indicators in Applying Plate Tectonics to Old Rocks*, J. Geol. *81*, 406–433.

CHANDRA, U. (1977), *Earthquakes of Peninsular India—A Seismotectonic Study*, Bull. Seismol. Soc. Am. *67*, 1387–1413.

DESSAI, A. G., and BERTRAND, H. (1995), *The "Panvel Flexure" along the Western Indian Continental Margin: An Extensional Fault Structure Related to Deccan Magmatism*, Tectonophysics *241*, 165–178.

FROHLICH, CLIFF, and DAVIS, SCOTT, D. (1993), *Teleseismic b Values; Or*, *Much Ado About 1.0*, J. Geophys. Res. *98*, 631–644.

GANGRADE, B. K., and ARORA, S. K. (1996), *Peninsular Seismicity: A Comprehensive Study from Regional Earthquake Data of Two Decades from Gauribidanur Seismic Array*, BARC Publ. no. BARC/1996/E/024.

GANGRADE, B. K., PRASAD, A. G. V., and SHARMA, R. D. (1987a), *Earthquakes from Peninsular India: Data from the Gauribidanur Seismic Array*, BARC Publ. no. 1347.

GANGRADE, B. K., PRASAD, A. G. V., and SHARMA, R. D. (1987b), *Earthquakes from Peninsular India: Data from the Gauribidanur Seismic Array for the Period January–December 1986*, BARC Publ. no. 1385.

GANGRADE, B. K., ARORA, S. K., PRASAD, A. G. V., and UNNIKRISHNAN, E. (1992), *Seismicity of Peninsular India Using Gauribidanur data for the period 1989–1991*, BARC Publ. no. BARC/1992/E/024.

GANGRADE, B. K., PRASAD, A. G. V., UNNIKRISHNAN, E., CHANDRASEKAR, B., SUBBARAMU, K. R., and SHARMA, R. D. (1989), *Earthquakes from Peninsular India: Data from the Gauribidanur Seismic Array for the Period January*, *1987–December*, *1988*, BARC Publ. no. 1454.

GANGRADE, B. K., ARORA, S. K., BASU, T. K., PRASAD, A. G. V., UNNIKRISHNAN, E., and MANOJ, KUMAR (1994), *Typical Seismicity of Peninsular India Based on Gauribidanur Array Data Obtained during the Two-year Period of 1992–1993*, BARC Publ. no. BARC/1994/E/040.

GUPTA, H. K. (1985), *The Present Status of Reservoir-induced Seismicity Investigations with Special Emphasis on Koyna Earthquakes*, Tectonophysics *118*, 257–279.

GUPTA, H. K. (1992), *Reservoir-induced Earthquakes*, Curr. Sci. *62*, 183–198.

GUPTA, H. K. (1993), *The Deadly Latur Earthquake*, Science *262*, 1666–1667.

GUPTA, H. K., and RASTOGI, B. K., *Dams and Earthquakes* (Amsterdam, Elsevier 1976).

HERRMANN, R. B. (1975), *The Use of Duration as a Measure of Seismic Moment and Magnitude*, Bull. Seismol. Soc. Am. *65*, 899–913.

KEBEDE, FEKADU, and KULHANEK, OTA (1994), *Spatial and Temporal Variations of b Values along the East African Rift System and the Southern Red Sea*, Phys. Earth Planet. Int. *83*, 249–264.

KHATTRI, K. N. (1994), *A Hypothesis for the Origin of Peninsular Seismicity*, Curr. Sci. *67*, 590–597.

KOLVANKAR, V. G., NADRE, V. N., ARORA, S. K., and RAO, D. S. (1992), *Development and Deployment of Radio Telemetered Seismic Network at Bhatsa*, Curr. Sci. *62*, 199–212.

KRISHNA BRAHMAM, N., and NEGI, J. G. (1973), *Rift Valleys Beneath Deccan Traps (India)*, Geophys. Res. Bull *11*, 207–237.

KRISHNA BRAHMAM, N., and KANUNGO, D. N. (1976), *Inference of Granitic Batholiths by Gravity Studies in South India*, J. Geol. Soc. Ind. *17*, 45–53.

LAY, THORNE, and WALLACE, TERRY C., *Modern Global Seismology* (Academic Press 1995) p. 384.

RAO, R. B. (1992), *Seismicity and Geodynamics of the Low to High-grade Transition Zone of Peninsular India*, Tectonophysics *201*, 175–185.

RAO, R. B., and RAO, S. P. (1984), *Historical Seismicity of Peninsular India*, Bull. Seismol. Soc. Am. *74* (6), 2519–2533.

RASTOGI, B. K. (1992a), *Seismotectonics Inferred from Earthquakes and Earthquake Sequences in India during the 1980s*, Curr. Sci. *62*, 101–108.

RASTOGI, B. K. (1992b), *Seismicity of India*, Lecture Notes vol. 1, Microearthquake Investigations, First SERC School on Seismology and Earthquake Processes, Hyderabad, December 11–31.

REAL, C. R., and TENG, TA-LIANG (1973), *Local Richter Magnitude and Total Signal Duration in Southern California*, Bull. Seismol. Soc. Am. *63*, 1089–1827.

SEEBER, L., EKSTRÖM, G., JAIN, S. K., MURTY, C. V. R., CHANDAK, N., and ARMBRUSTER, J. J. (1996), *The 1993 Killari Earthquake in Central India: A New Fault in Mesozoic Basalt Flows?*, J. Geophys. Res. *101*, 8543–8560.

VALDIYA, K. S. (1973), *Tectonic Framework of India: A Review and Interpretation of Recent Structural and Tectonic Studies*, Geophys. Res. Bull. *11*, 79–114.

VALDIYA, K. S. (1989), *Neotectonic Implications of Collision of Indian and Asian Plates*, Ind. J. Geol. *61*, 1–13.

(Received June 1, 1999, accepted March 1, 2000)